



UNIVERSITY OF GOTHENBURG

This is an author produced version of a paper published in **Climate Dynamics**

This paper has been peer-reviewed but does not include the final publisher proof-corrections or journal pagination.

Citation for the published paper:

Christian Stranne, Göran Björck:

On the Arctic Ocean ice thickness response to changes in the external forcing

Climate Dynamics, 39 (12) s. 3007-3018

<http://dx.doi.org/10.1007/s00382-011-1275-y>

Access to the published version may require subscription. Published with permission from: **Springer**

GUP

Gothenburg University Publications

<http://gup.ub.gu.se/gup/>

On the Arctic Ocean ice thickness response to changes in the external forcing

Christian Stranne^{ab} and Göran Björk^a

^a University of Gothenburg

Dept. of Earth Sciences

Box 460

SE-405 30 Göteborg

Sweden

^b Corresponding author

Phone: +46 (0)31 7862874

Mobile: +46 (0)706-476154

email: christian.stranne@gvc.gu.se

Abstract

Submarine and satellite observations show that the Arctic Ocean ice cover has undergone a large thickness reduction and a decrease in the areal extent during the last decades. Here the response of the Arctic Ocean ice cover to changes in the poleward atmospheric energy transport, F_{wall} , is investigated using coupled atmosphere-ice-ocean column models. Two models with highly different complexity are used in order to illustrate the importance of different internal processes and the results highlight the dramatic effects of the negative ice thickness – ice volume export feedback and the positive surface albedo feedback. The steady state ice thickness as a function of F_{wall} is determined for various model setups and defines what we call ice thickness response curves. When a variable surface albedo and snow precipitation is included, a complex response curve appears with two distinct regimes: a perennial ice cover regime with a fairly linear response and a less responsive seasonal ice cover regime. The two regimes are separated by a steep transition associated with surface albedo feedback. The associated hysteresis is however small, indicating that the Arctic climate system does not have an irreversible tipping point behaviour related to the surface albedo feedback. The results are discussed in the context of the recent reduction of the Arctic sea ice cover. A new mechanism related to regional and temporal variations of the ice

divergence within the Arctic Ocean is presented as an explanation for the observed regional variation of the ice thickness reduction. Our results further suggest that the recent reduction in areal ice extent and loss of multiyear ice is related to the albedo dependent transition between seasonal and perennial ice i.e. large areas of the Arctic Ocean that has previously been dominated by multiyear ice might have been pushed below a critical mean ice thickness, corresponding to the above mentioned transition, and into a state dominated by seasonal ice.

Keywords

Arctic Ocean, sea ice, sensitivity, divergence, albedo feedback, ice export, tipping point

1 Introduction

The Arctic sea ice cover has been reduced substantially over the last decades both in terms of area, with a decline in the summer sea ice extent of more than 10 % per decade between 1979 – 2007 (Stroeve et al. 2008), and in terms of volume as indicated by an observed average thinning of more than 1.5 m since the 80s (Rothrock et al. 1999; Tucker et al. 2001; Kwok and Rothrock 2009). The ice reduction has also been accompanied by a significant loss of multiyear ice in winter from a coverage of ~70% of the Arctic Ocean area two decades ago to a present day coverage of ~50% (Johannessen et al. 1999; Comiso 2002; Kwok 2009). A general feature of the declining Arctic Ocean ice cover is that the thickness reduction in regions with thick ice have been greater compared to regions with thinner ice as was noted by Bitz and Roe (2004) (hereafter abbreviated as B&R). They argued that the observed relation between thickness reduction and initial ice thickness can be explained by the thermodynamic properties of sea ice through the ice thickness – ice growth rate feedback mechanism which is related to the fact that thin ice grows much faster than thick ice. B&R based their analysis on a theoretical relation between ice thickness and sensitivity to forcing perturbations using a simplified Analytical version of the Toy Model (ATM) developed by Thorndike (1992), and showed that observations as well as the results of several general circulation model experiments match the theoretical ice thickness response fairly well.

In this study we make a more extensive investigation of the response properties of the Arctic sea ice by considering some additional processes that are not included in the ATM with the aim to increase the realism. The main additional processes that are assessed are *i)* an ice thickness distribution, *ii)* ice export, *iii)* snow precipitation and *iv)* a variable surface albedo parameterization. The ice thickness response to changes in the atmospheric forcing, when these processes are added, becomes rather different compared to the original ATM response and our results indicate that regional and temporal variations of the ice divergence and also the albedo feedback play an important role in explaining the observed ice thickness reduction.

We investigate the response properties of the Arctic Ocean by the means of idealized experiments with coupled ocean-ice-atmosphere column models. A similar approach has been employed in several previous studies (e.g. Maykut 1982; Bjork 1992; Thorndike 1992; Bitz and Roe 2004; Soderkvist and Bjork 2004; Eisenman and Wettlaufer 2009; Curry et al. 2001).

This kind of idealized studies, where parts of the climate system are isolated in a controlled way, have the potential to provide knowledge of the system properties such as sensitivities to forcing perturbations and feedbacks and serves therefore as an important compliment to coupled general circulation model experiments.

In this study we focus on the ice thickness response to changes in the meridional atmospheric heat flux, F_{wall} (defined as the net energy flux across the 70°N latitude circle). This quantity is a dominant term in the overall Arctic heat budget along with solar radiation and the long wave radiation back to space (Thorndike 1992). Since F_{wall} is closely related to the atmospheric circulation pattern it is natural to use as an independent variable forcing quantity. The annual incoming solar radiation is nearly constant and the radiation back to space is an internal quantity in this respect which is highly dependent on F_{wall} . When considering the observed reduction of the ice cover over the last decades, changes in the atmospheric circulation and thereby F_{wall} has likely played a large role with e.g. an observed correlation between increased air temperature and increased F_{wall} (Graversen et al. 2008). There are also theoretical as well as modelling results linking increased global CO₂ levels with an increased F_{wall} (e.g. Cai 2006; Alexeev et al. 2005; Rind 1987). Increasing atmospheric temperatures has then a direct effect on the ice cover through increased downward long wave radiation.

2 Model descriptions

2.1 The Analytical Toy Model (ATM)

The basic properties of the Arctic ice cover were described in the Toy Model developed by Thorndike (1992). Following B&R we use the same simplified analytical version of the Toy Model to calculate the steady state ice thickness as a function of the radiative forcing (in this case F_{wall}) defined as:

$$G(H_{ice}) = \frac{\tau}{L} \left[\frac{A + BT(H_{ice})}{n_w} - \frac{F_{wall}}{2} - F_w \right] \quad (1)$$

$$M = \frac{\tau}{L} \left[-\frac{A}{n_s} + \frac{F_{wall}}{2} + F_w + (1 - \alpha)F_{sw} \right] \quad (2)$$

$$T(H_{ice}) = \left(\frac{n_w H_{ice}}{kn_w + BH_{ice}} \right) \left(-\frac{A}{n_w} + \frac{F_{wall}}{2} \right) \quad (3)$$

where G is annual growth, M is the annual melt, H_{ice} is the annual mean steady state ice thickness, τ the length of the growing/melting season, L the heat of fusion, T the ice surface temperature, n_w/n_s the atmospheric optical thickness during winter/summer, F_w the oceanic heat flux, α the surface albedo and k the thermal conductivity of ice. A and B are coefficients representing a linearized Stefan Boltzmann's radiation law. Eq. (3) gives the relation between ice thickness and surface temperature during winter. The steady state ice thickness H_{ice} is obtained by solving

$$G(H_{ice}) - M = 0 \quad (4)$$

representing a balance between growth and melt over the year. For clarity, the functional dependence of G on H_{ice} through T is highlighted in these equations. The parameter values are given in Table 1.

While B&R studied the ice thickness response by making perturbations on the total downwelling long wave, LW, radiation we will instead consider perturbations in F_{wall} . In this simplified model 50 % of F_{wall} is lost directly to space while the rest radiates down at the surface. A perturbation of 4 Wm^{-2} of the downwelling LW radiation employed by B&R (corresponding crudely to a doubling in the atmospheric CO_2 content) is thus equivalent to an 8 Wm^{-2} perturbation in F_{wall} .

2.2 The Coupled Column Arctic Model (CCAM)

The other model used in this study (CCAM) is much more complex than the ATM including a full radiation scheme in the atmosphere and an ice cover represented by an ice thickness distribution. The atmospheric part of the CCAM is a standalone version of the column radiation code employed by the NCAR Community Climate Model (CCM3), (Collins et al. 2006). It has a vertical grid of 18 layers. A convective adjustment scheme and an internal heat source in each layer, corresponding to the external energy supply at the vertical boundary (F_{wall}), are added in the present application. F_{wall} follows a climatological cycle calculated from the NCEP reanalysis data set using the algorithm presented by Overland and Turet (1994) with a baseline annual mean F_{wall} of approximately 100 Wm^{-2} , see Table 2. Clouds occupy a certain fraction, CF of the sky at three different levels and follows an annual climatological cycle calculated from the ISCCP D2 dataset (Rossow and Duenas 2004), see Table 2.

The model ice cover is separated into a number of ice categories of different thicknesses (i.e. the ice thickness distribution). Each category may also have a snow cover on top (see Bjork 1997 for a comprehensive description). The ocean part is a column model with an active surface mixed layer controlled by mechanical mixing due to ice motion together with heat and salt fluxes at the surface. The stratification is also controlled by advective processes due to Bering Strait inflow, river discharge, geostrophical outflow, and a hypothetical shelf circulation (Bjork 1989). The surface is coupled with the atmosphere such that heat fluxes are computed individually for each ice category, including open water. The single column atmosphere is then updated using area weighted heat fluxes. The time step in the model is two hours.

3 Results

The steady state ice thickness as a function of F_{wall} is determined for various model setups and defines what we call ice thickness response curves. The gradient of a response curve is then a measure of the sensitivity of the ice cover to forcing perturbations (a steeper slope means higher sensitivity).

3.1 The ATM response curve

First we look at the steady state ice thickness dependence on F_{wall} for a slab ice cover with a single thickness, no snow precipitation and constant ice albedo, corresponding to the analytical version of the Toy Model, Eqs. (1) – (4). The relation between ice thickness and F_{wall} is non-linear with decreasing ice thickness with increasing F_{wall} (black curve Fig. 1 a). The response implies that thick ice is much more sensitive to changes in F_{wall} than thin ice, a mechanism known as the ice thickness - growth rate feedback (Gordon and OFarrell 1997; Zhang et al. 2000; L'Heveder and Houssais 2001; Bitz and Roe 2004). This feedback is related to the fact that thick ice grows substantially slower than thin ice (a non-linear relation) as was first discussed by Stefan (1890). When the ice cover is in steady state, the summer ice melt must be equal to the growth during winter. As a consequence, an increase in the summer melt due to some forcing perturbation must be compensated by increased ice growth. If the ice cover is thick, a relatively large reduction of the ice thickness is needed in order to obtain the extra growth. In contrast, for thin ice, only a small thickness reduction is sufficient to obtain the same additional growth.

It should be noted that the very thick ice ($> \sim 10$ m) for low F_{wall} values in the ATM response curves may not be realistic since Eqs. (1) – (3) does not hold for such thick ice. By using the

more realistic numerical version of the Toy Model, it can be shown that the maximum ice thickness is ~ 10 m at which point the model comes into a state where the freezing/warming periods cover the entire year leaving no time for growth/melting.

3.2 The influence of an ice thickness distribution

The next experiment is meant to mimic the Toy model as closely as possible while the effect of an ice thickness distribution (ITD) is also included. In order to achieve this we use the more complex column model, CCAM where the ice model includes ~ 50 ice thickness categories with different thickness and area coverage which together constitutes the ice thickness distribution. Similar to the Toy model set up, the surface albedo is kept constant and equal for all categories. In order to generate a thickness distribution it is necessary to introduce deformation of the ice cover which is described by two separate processes: ridging and horizontal ice divergence (see Bjork 1992 for an extensive description). In this model setup an ITD is created through the introduction of a specific amount of ridging type of deformation without any net divergence. An area equivalent to 40 % of the basin per year is forced open through a constant piling of thin ice categories into thicker ridged categories. The ridging process thus creates open water and redistributes ice from the thinner to the thicker part of the distribution while conserving the ice volume. The effect of net divergence is treated later. Note that we compare a highly simplified analytical model to a model including a much more sophisticated treatment of atmospheric radiation, a fully coupled ocean model and a more developed ice model including thermal inertia and treatment of brine pockets. This means that we are not exclusively adding the effect of an ITD here but also a more realistic treatment of the atmospheric radiation and the ocean heat flux, although we mainly discuss the difference between the response curves in terms of ITD effects.

The ice thickness response to F_{wall} perturbations is relatively similar to the ATM in this case (Fig. 1a) but there are some important differences. A general effect of the introduction of an ITD is an increase of the equilibrium ice thickness over the larger part of the F_{wall} interval. This is caused by the ridging process which continuously facilitates categories with thicker ice together with open water and thin ice categories, due to the constant development of leads. Since the thin portion of the ice cover has much larger growth than the thick part this leads to an increase of the total growth, compared to a single ice floe with the same thickness as the distribution mean. This property of the ITD has been demonstrated earlier by (Holland et al. 2001; Maykut 1982; Bitz et al. 2001; Holland et al. 2006). It should be noted however, that

this effect is maximal when using a constant surface albedo. A variable surface albedo, dependent on the surface properties (e.g. snow, bare ice and open water) will, at least to some extent, cancel out the effect of increased ice growth during winter by enhanced absorption of shortwave radiation in leads and over thin ice categories during summer as was shown by Björk (1997).

3.3 The influence of ice export and divergence

The ice export from the Arctic Ocean occurs mainly through Fram Strait and is an important sink term in the Arctic ice mass balance. Associated with the ice export there must be a net divergence of the ice cover in the basin interior generating areas of open water which corresponds to the area of ice lost by export. Using a time series over 29 years of passive microwave brightness temperature and ice concentration fields, Kwok (2009) estimated the annual mean ice area export to around $7 \cdot 10^5 \text{ km}^2 \text{ year}^{-1}$ and the mean volume transport to around $2200 \text{ km}^3 \text{ year}^{-1}$. The ice export out of the Arctic Ocean represents a thickness loss of $\sim 0.3 \text{ m year}^{-1}$ and as a consequence, in steady state, the net ice production must exceed the annual melt by an equal amount. Analogous with the mechanism behind the ice thickness – growth rate feedback (section 3.1), this new sink term in the ice mass budget implies that the ice thickness needs to be reduced until the growth rate increase compensates for the export. Consequently, the addition of ice export should in general lead to thinner equilibrium ice thickness.

In the following experiments the albedo is kept constant while ice export is introduced to both the ATM and the CCAM. We use the divergence D , to represent the areal export defined as $D = A_{ex}/A_B$ where A_{ex} is the areal export and A_B the area of the Arctic Ocean ($A_B = 0.78 \cdot 10^{13} \text{ m}^2$). The ice volume export, Q_{ice} can then be expressed in terms of divergence and ice thickness:

$$Q_{ice} = DA_B H_{ice} \quad (5)$$

where H_{ice} denotes the ice thickness (averaged over the ITD in the CCAM). We use two different divergence formulations, DF_1 and DF_2 : The DF_1 case has a specified constant volume export, $Q_{ice} = 1 \cdot 10^5 \text{ m}^3/\text{s}$, which implies that the divergence is a function of ice thickness according to Eq. (5). The DF_2 case has a constant annual mean divergence with $D = 4.6 \cdot 10^{-9} \text{ s}^{-1}$ corresponding to 14.5 \% yr^{-1} of the total basin area (taken from Kwok and Rothrock (1999)) and is thus independent of the ice thickness. Note that Q_{ice} becomes a linear function of ice thickness according to Eq. (5) in the DF_2 case.

In the ATM model the ice export corresponds to an additional sink term in Eq. (4).

$$G(H_{ice}) - M - E = 0 \quad (6)$$

where E is the annual ice volume export per square meter given by

$$E = \begin{cases} 2\tau Q_{ice} / A_B & , DF_1 \\ 2\tau D H_{ice} / A_B & , DF_2 \end{cases} \quad (7)$$

For the DF_2 case in the CCAM model, the divergence follows a fixed seasonal cycle around the annual mean D with significantly less divergence during summer (Kwok and Rothrock 1999). The divergence is always based on the ice covered fraction of the basin, meaning that a certain percentage of the ice leaves the area per unit time, and is therefore independent of the amount of open water.

When introducing a constant ice volume export (DF_1 case) the tendency of the export is to decrease the equilibrium ice thickness and to stabilize the ice cover, making it less responsive to forcing perturbations (Fig. 1b). As mentioned above the inclusion of ice export calls for an increased net ice growth in order to keep the mass balance. However due to the nonlinear relation between growth rate and ice thickness, thick ice needs to be reduced more than thinner ice in order to reach the same growth rate increase (the ice thickness – growth rate feedback). The response curve therefore becomes more linear compared to the no ice export cases and the tendency is the same for both the ATM and the CCAM models.

Having the horizontal divergence independent of ice thickness (DF_2 case), (Fig. 1c), gives a rather different response compared to the previous cases. The response curves are now essentially linear, especially for the CCAM model which has a constant slope of about 1 m ice thickness reduction per 10 Wm^{-2} increase of F_{wall} . The greatly reduced ice thickness sensitivity for the DF_2 case is due to the strong negative ice thickness – ice volume export feedback, as indicated by Eq. (5). It is remarkable that the response curves are so similar for the two models which actually indicates that the very simple ATM model includes the most important processes in a realistic way.

It is in place here with a discussion of the realism of the two ice export cases. A constant ice volume export (the DF_1 case) for different thicknesses of the outflowing ice is not very

realistic since there are no natural mechanisms keeping $A_{ex} \cdot H_{ice}$ constant. A constant divergence (the DF_2 case) on the other hand implies that the net divergence is independent of the ice thickness and thus assuming that the prevailing wind systems in the Arctic control the areal ice export alone. In reality there is a dynamic coupling between ice mobility and ice thickness such that thin ice is more easily exported than thick ice. This dynamic effect comes into play when the internal ice stresses become comparable to the dynamic forcing caused by wind and ocean currents. Observations indicate however that the areal ice export has a direct response to the wind forcing and that it correlates well with the prevailing pressure gradients over Fram Strait and the NAO (e.g. Hilmer and Jung 2000; Kwok and Rothrock 1999; Kwok 2009). This suggests that the areal ice export is a strong function of wind forcing and, at least to the first order, independent of ice thickness under present day 2 - 3.5 m ice conditions. Moreover, no clear trends in the areal ice export during the last three decades has been found (Kwok 2009) which suggests that areal ice export has not been affected by the recent Arctic ice thickness reduction. The ice velocities has in fact increased in the Fram Strait during the last years of the study but this has been compensated by decreasing ice concentrations resulting in a small net effect of the ice area export (Kwok 2009). The increased ice export velocities at Fram Strait are however a consequence of a positive trend in the gradient of cross-strait sea level pressure and are thus probably not directly associated with the general thinning of the Arctic ice cover.

The DF_2 case seems to be reasonable for the observed ice conditions during the satellite era (from the early 80's to present). For hypothetically more severe ice conditions, with much thicker ice, the internal ice stress becomes more important and especially the increasing shear strength might lead to sea ice arching in the export passages which in turn could reduce the ice export significantly (Hibler et al. 2006). We therefore introduce a third divergence formulation, DF_3 taking the ice thickness into consideration. Here the divergence is reduced with increasing H_{ice} in approximate accordance with Hibler et al. (2006) while still following the annual climatological cycle of Kwok and Rothrock (1999), see Appendix for details. The DF_3 case gives a similar result compared to the constant divergence case (the DF_2 case) for thin ice while there is a sharp transition for ice thicker than ~ 5 m where the internal stress becomes so strong that the response curve closely follows the zero volume export curve from Fig. 1a (reproduced in Fig. 2). A huge hysteresis exerts a large asymmetrical affect on the ice response with a tipping point at about $F_{wall} = 85 \text{ W/m}^2$ (with a rapid transition from 10 to 5 m) when “coming out of a cold era” compared to a tipping point at about $F_{wall} = 72 \text{ W/m}^2$ (with a

rapid transition from 7 m to 17 m) when “entering a cold era”. Very similar dual stability modes were also obtained by Hibler et al. (2006).

The overall effect of ice export is a tendency to reduce the equilibrium ice thickness and to stabilize the ice cover, making it less responsive to forcing perturbations. This is a general result which holds for both the ATM and the CCAM models regardless of the export formulation, at least for relatively thin ice with no dynamic interaction. This result is in accordance with Vavrus (1999) who demonstrates that ice transport gives rise to negative feedbacks with respect to sea ice thickness for both positive and negative forcing perturbations. By invoking the feedback between ice strength and ice export (the DF_3 case), B&R suggested that ice export instead might increase the ice thickness sensitivity. Their conclusion was reached by quoting earlier work by Hibler and Hutchings (2002) who proposed a transition between the low and high export states of the Arctic (the steep transition of the DF_3 case, Fig. 2) at an ice thickness of around 3 m, meaning that this feedback would become relevant for present day ice conditions. However as mentioned above, ice export observations indicate that, at least during the satellite era, the dynamic coupling between export and ice strength has been marginal. This is also supported by the more recent modelling efforts by Hibler et al. (2006).

It might be difficult to find a detailed and realistic description of the actual export - thickness dependence and it is not the purpose of the present study to go particularly deep into this subject. Suffice to say that dynamic effects seem to be of minor importance for the typical basin average thickness of 2 - 3.5 m that has been observed during the last decades. The choice of ice export formulation will be more critical when modelling a colder climate with much thicker ice. What proves to be of greater importance for the present day relatively thin ice conditions, especially when considering possible future global warming, is the surface albedo feedback which is treated in the next section.

3.4 The influence of variable surface albedo and snow precipitation

The following computations including variable surface albedo and snow precipitation are only made with the CCAM model since the ATM formulation does not support a snow cover.

The presence of a snow cover on sea-ice can have a substantial effect on the equilibrium ice thickness. The insulating property of snow reduces effectively the heat loss from the ocean

during the winter season and thus limits the ice growth. During the early melting period however, a snow cover has the opposite effect on the equilibrium ice thickness through the much higher albedo ($\sim 90\%$) compared to bare sea ice ($\sim 60\%$) and open water ($\sim 10\%$). The high snow albedo reduces the melting and thereby tends to increase the equilibrium ice thickness when a snow cover is present. An expected effect of adding snow precipitation is thus a dampening of the annual ice thickness variation amplitude. Snow precipitation is however by large an unknown quantity which is not only difficult to model, due to the not well understood cloud and water vapour dynamics of the Arctic atmosphere (e.g. Verlinde et al. 2007; Soden and Held 2006), but also hard to validate due to the scarce precipitation data available for the central Arctic. Nevertheless, by adding climatological precipitation to the CCAM we can demonstrate at least the qualitative influence of snow precipitation on the ice thickness response curve. The climatological precipitation is calculated from The Arctic Meteorology and Climate Atlas (Arctic Climatology Project, 2000) where only area weighted ocean grid cells has been considered. The climatological precipitation in snow equivalent, S_{prec} was trimmed by a factor 1.5 so that the maximum snow depth equals 0.3 m in our baseline F_{wall} forcing case, see Table 2. The insulating property of snow alone (still keeping the albedo constant) is shown in Fig. 3a. It is evident that the insulating property dominates over the constant albedo, giving rise to thinner ice when precipitation is included in the model. When a dynamic albedo parameterization is introduced however, the competing high albedo property of snow becomes dominant and we get a thicker ice cover when snow precipitation is added (Fig. 3b).

The ice albedo α_{ice} , employed in this study is taken from Maykut (1982) and is a function of ice thickness according to

$$\alpha_{ice} = \min(0.08 + 0.44 H_{ice}^{0.28}, 0.64)$$

and the snow albedo, α_{snow} follows an annual climatological cycle (Table 2).

The inclusion of a more realistic and variable surface albedo gives a more complicated response curve including a fast transition into a seasonal ice cover (i.e. ice free summers), (Fig. 3b). The response can now be separated into three regimes: a regime with perennial ice and a close to linear response, a transitional regime from a perennial to a seasonal ice cover and a less responsive seasonal ice regime. This type of transitional response was also described and discussed for a similar model set-up in the extensive study on the Arctic sea ice

response by Björk and Söderkvist (2002). The albedo feedback generates a strong thickness dependence when the system is close to the transition between seasonal and perennial ice. In our case this transitional regime is located around an ice thickness of 2 m, (Fig. 3b).

4 Discussion

The main purpose of this paper has been to show how the ice thickness sensitivity to changes in the atmospheric forcing, as here exemplified by F_{wall} , is affected when including a higher degree of realism compared to a simple slab ice cover. It is then interesting to discuss how our results relate to observations. One point of contact between this study and observations is the observed tendency that thick ice has decreased more in thickness than thin ice as seen from submarine data and several model studies (see B&R). An overall result from the present study is that dynamic ice processes as well as the surface albedo feedback process exert a considerable influence on the ice thickness response properties and that a more realistic response curve likely has a shape similar to the one in Fig. 3b (with snow) rather than the continuous response in Fig. 1a. The CCAM response curve is however essentially linear over the perennial ice thickness regime which indicates a constant ice thickness sensitivity, independent of the initial ice thickness. So how can this result be consistent with the thickness dependent sensitivity as indicated by both submarine observations and several model studies?

One possible explanation is that the observed ice thickness response is related to regional and temporal variations of the horizontal divergence within the Arctic Ocean. It is clear that there must be an overall net divergence when averaged over the basin (related to the net ice area export) but there could well be regions within the basin with generally larger or smaller divergence compared to the basin average. Such regional differences in the divergence are straightforward to simulate with the present CCAM model assuming that the atmospheric forcing and oceanic conditions are similar for the different regions. Response curves for different divergences are shown in Fig. 4 which then should represent different regions of the Arctic Ocean under the assumption above. The calculated average divergence field, based on gridded velocity field data from the IABP buoy program (Rigor, 2002), shows indeed a clear pattern of regional variations (Fig. 5a). The divergence is highest in the outflow region towards Fram Strait and north-western Barents Sea. In the interior basin there is a local maximum in the central Canadian Basin while the divergence is reduced towards the coasts and also changes sign in some regions indicating net convergence. According to Fig. 4, a small amount of divergence is sufficient in order to get a close to linear perennial ice cover

response which means that we would not expect to have a non-linear ice thickness – growth rate feedback response (seen in Fig. 1a) even in low divergence zones of the Arctic Ocean. However, an area with low divergence will not only have thicker ice but would also be more sensitive to forcing perturbations compared to areas with high divergence (as indicated by the steeper slope of the response curve in Fig. 4). This indirect relation between ice thickness and ice thickness sensitivity, with the variable divergence serving as the link in between, might therefore explain the observed initial ice thickness – thickness reduction relation. Studying Fig. 5a it is however clear that no simple relation exists between the divergence field and the typical observed ice thickness field. If only taking the ice thickness dependence on divergence into account, the ice cover would be thickest along the rim of the basin and thinner in the central parts (and very thin close to Fram Strait) which is not in accordance with ice thickness observations. The actual ice cover is in fact controlled by several additional processes. For instance, areas dominated by strong advection, as in the vicinity of Fram Strait, are strongly influenced by the upstream ice conditions since the ice cover will not have time to adjust thermodynamically to the local forcing. There are also regional differences in the thermodynamic forcing such as the difference in solar incidence (a difference at the top of the atmosphere of about 13 Wm^{-2} or 8 % between 75 and 90°N) and differences in the atmospheric and the oceanic heat advection. An area which is likely in a quasi-equilibrium state is the region north of the Canadian archipelago where the typical divergence is low and the residence time relatively long. This area is known to have thick ice and the thickness reduction has also been relatively large (Kwok and Rothrock 2009).

In Fig. 5b the linear trend of the annual mean divergence for each grid cell over time between 1979 and 2007 is shown. Although the resulting field is smooth with well defined regions of positive and negative trends and with continuous transitions in between them, one has to be somewhat cautious when interpreting these trends due to possible spatial and temporal inhomogenities in the data set. The largest positive trend (close to $0.4 \cdot 10^{-7} \text{ s}^{-1} \text{ year}^{-1}$) found in the area north of Greenland goes from values around $-5 \cdot 10^{-7} \text{ s}^{-1}$ in the early 80's to typical values above $5 \cdot 10^{-7} \text{ s}^{-1}$ some 30 years later. The negative trends in the northern Barents Sea and in the central Canadian Basin are about half as strong. A logical assumption is that the general ice thickness reduction in the Arctic Ocean has been affected by these quite substantial changes in the divergence over time such that regions with positive trends would experience a larger thickness reduction compared to regions with negative trends, due to the direct link between divergence (local ice area export) and ice thickness as shown in Fig. 4.

Assume, as an idealized example, that there has been an increasing but spatially uniform thermodynamic atmospheric forcing over the period, tending to give a uniform thickness reduction. Then adding the effect of regionally variable trends of divergence would give a larger ice reduction in e.g. the area north of Greenland (having a positive trend) and less ice reduction in the Beaufort Sea (having a negative trend). Indeed this pattern fits very well with the observed regional ice thickness reduction as reported by Kwok and Rothrock (2009) showing smaller ice reduction in the Beaufort- and Chuckchi Sea areas compared to the area north of Greenland, the North Pole region and the Eastern Arctic. If the regionally varying divergence trends is the main process responsible for the observed regional variations of the ice thickness reduction, it should be noted that the observed initial thickness – thickness reduction relation would be coincidental since the divergence is a strong function of the atmospheric circulation and thus not directly associated with the initial ice thickness.

Moving on to the surface albedo feedback, we have already concluded that it plays an overall important role in terms of response properties of the Arctic sea ice cover, a conclusion which is consistent with several other studies (e.g. Hall 2004; Holland and Bitz 2003; Winton 2006). The transitional regime, created by the albedo feedback, constitutes a highly nonlinear feature on the response curve which means that when the perennial ice cover approaches a threshold in the average ice thickness (in our study ~ 2 m) it becomes exceedingly sensitive to positive forcing perturbations. The associated hysteresis when going back from seasonal to perennial ice is small ($< 1 \text{ Wm}^{-2}$, not shown) and thus one should expect a large interannual variability of the perennial ice area extent in regions of the Arctic Ocean where the ice cover lies close to the transition, since very small annual variations in the atmospheric forcing is sufficient to push the ice cover from perennial to seasonal ice or vice versa. This is also an observed feature of the Arctic sea ice cover where the annual minimum ice extent sometimes varies by well over one million square kilometers between two consecutive years (Stroeve et al. 2007). Furthermore, the small hysteresis implies that the Arctic climate system does not have an irreversible tipping point behavior associated with the surface albedo feedback, a result consistent with column model simulations (Eisenman and Wettlaufer 2009) and recent GCM simulations (e.g. Armour et al. 2011; Tietsche et al. 2011). Our results further implies that the sudden reduction in multiyear ice that has been reported (Comiso 2002; Johannessen et al. 1999; Kwok and Rothrock 2009) can, at least partly, be explained by the surface albedo feedback. Large areas of the Arctic Ocean that has previously been dominated by multiyear ice might have been pushed below a critical mean ice thickness and into a state dominated by

seasonal ice. The exact shape of the transitional regime might however be subject to large uncertainties. For instance, it is likely dependent on the details of the albedo parameterization and on the ridging scheme. Since all atmospheric cloud and water vapour parameters are prescribed (following annual climatological cycles) in the CCAM we do not catch the feedbacks associated with the water vapour and cloud formation processes here. There are studies suggesting that the overall effect constitutes a positive feedback in terms of sea surface temperature (Webb et al. 2006; Holland and Bitz 2003) but there are large uncertainties associated with simulating Arctic clouds (e.g. Wyser et al. 2008) and there is no consensus in the scientific community regarding the net effect of the negative cloud albedo feedback and the positive infrared radiation feedback (Cai and Lu 2010). Although there are uncertainties regarding the overall response properties of the Arctic sea ice, our model results suggest that the albedo feedback mechanism is at least partly responsible for the loss of multiyear ice over the last decades. A more focused modelling effort on the details of this transitional regime using a full 2D ice model (including advective and regional effects) would however be needed in order to quantify the loss of multiyear ice due to the surface albedo feedback.

We note also that the transitional regime created by the surface albedo feedback can explain part of the above discussed initial ice thickness – thickness reduction relation. The transition represents a nonlinear response where perennial ice approaching the transition will be exceedingly sensitive to positive forcing perturbations while areas dominated by seasonal ice will remain relatively insensitive. This means that part of the observed thickness dependent response (the part involving relatively thin ice) can be explained by the fact that some portion of the perennial ice cover has been transformed into seasonal ice.

To sum up, we have illustrated the quite significant effects of the negative ice thickness – ice volume export feedback and the positive surface albedo feedback in terms of Arctic sea ice thickness sensitivity. We have also shown that there is a relation between divergence and ice thickness and that this mechanism has the potential to explain the observed regional variations of the sea ice thickness reduction in the Arctic. Our model results further suggest that the Arctic climate system does not have an irreversible tipping point behaviour associated with the surface albedo feedback.

5 Appendix

We base this divergence formulation (DF_3) on an approximate version of the ice export - ice thickness relation, $Q'_{ice} = f(H_{ice})$, (Fig. A1a), presented by Hibler et al. (2006, their Fig. 7a). The observed annual cycle of the divergence as reported by Kwok and Rothrock (1999) is, at least to the first order, related to the prevailing wind systems over Fram Strait. Thus we keep the seasonal cycle of the divergence by using a normalized ice thickness factor, K_{ice} in this formulation. K_{ice} is obtained by dividing Q'_{ice} by the ice thickness Eq. (A1) and then normalizing so that an ice thickness of 2.5 m has K_{ice} equal to one Eq. (A2), (Fig. A1b). The ice thickness factor is also set to one for ice thinner than 2.5 m assuming that the ice export is purely wind driven and thus unaffected by the internal ice stress.

$$A'_{\text{exp}} = \frac{f(H_{ice})}{H_{ice}} \quad (\text{A1})$$

$$K_{ice} = \frac{A'_{\text{exp}}}{A'_{\text{exp}}(H_{ice} = 2.5)} \quad (\text{A2})$$

The ice volume export in the DF_3 case is then given by

$$Q_{ice} = K_{ice} D A_B H_{ice} \quad (\text{A3})$$

Acknowledgements

This work was funded by the Swedish Research Council VR (contract 621-2007-3836). We thank Anna Wåhlin and three anonymous reviewers for valuable and constructive comments on the manuscript. We also thank Ignatius Rigor, Cecilia Bitz and Yanling Yu for assistance with observational data.

References

- Stroeve, J. ., M. Serreze, S. Drobot, S. Gearheard, M. Holland, J. Maslanik, W. Meier, and T. Scambos (2008), Arctic Sea Ice Extent Plummetts in 2007, *Eos Trans. AGU*, 89(2), doi:10.1029/2008EO020001.
- Rigor, I. 2002. *IABP drifting buoy, pressure, temperature, position, and interpolated ice velocity*. Compiled by the Polar Science Center, Applied Physics Laboratory, University of Washington, Seattle, in association with NSIDC. Boulder, CO: National Snow and Ice Data Center. Digital media.
- Hibler, W. D., and J. K. Hutchings, 2002: Multiple equilibrium arctic ice cover states induced by ice mechanics. *Ice in the Environment: Proc. of the 16th IAHR Int. Symp. on Ice*, Dunedin, New Zealand, IAHR, 228–237.
- Arctic Climatology Project. 2000. Environmental Working Group Arctic meteorology and climate atlas. Edited by F. Fetterer and V. Radionov. Boulder, CO: National Snow and Ice Data Center.
- Alexeev VA, Langen PL, Bates JR (2005) Polar amplification of surface warming on an aquaplanet in "ghost forcing" experiments without sea ice feedbacks. *Clim Dynam* 24 (7-8):655-666. doi:10.1007/s00382-005-0018-3
- Armour KC, Eisenman I, Blanchard-Wrigglesworth E, McCusker KE, Bitz CM (2011) The reversibility of sea ice loss in a state-of-the-art climate model. *Geophys Res Lett* 38. doi:10.1029/2011GL048739
- Bitz CM, Holland MM, Weaver AJ, Eby M (2001) Simulating the ice-thickness distribution in a coupled climate model. *J Geophys Res-Oceans* 106 (C2):2441-2463
- Bitz CM, Roe GH (2004) A mechanism for the high rate of sea ice thinning in the Arctic Ocean. *J Climate* 17 (18):3623-3632
- Bjork G (1989) A One-Dimensional Time-Dependent Model for the Vertical Stratification of the Upper Arctic Ocean. *J Phys Oceanogr* 19 (1):52-67
- Bjork G (1992) On the Response of the Equilibrium Thickness Distribution of Sea Ice to Ice Export, Mechanical Deformation, and Thermal Forcing with Application to the Arctic-Ocean. *J Geophys Res-Oceans* 97 (C7):11287-11298
- Bjork G (1997) The relation between ice deformation, oceanic heat flux, and the ice thickness distribution in the Arctic Ocean. *J Geophys Res-Oceans* 102 (C8):18681-18698
- Bjork G, Soderkvist J (2002) Dependence of the Arctic Ocean ice thickness distribution on the poleward energy flux in the atmosphere. *J Geophys Res-Oceans* 107 (C10). doi:10.1029/2000JC000723
- Cai M (2006) Dynamical greenhouse-plus feedback and polar warming amplification. Part I: A dry radiative-transportive climate model. *Clim Dynam* 26 (7-8):661-675. doi:10.1007/s00382-005-0104-6
- Cai M, Lu JH (2010) Quantifying contributions to polar warming amplification in an idealized coupled general circulation model. *Clim Dynam* 34 (5):669-687. doi:10.1007/s00382-009-0673-x

- Collins WD, Rasch PJ, Boville BA, Hack JJ, McCaa JR, Williamson DL, Briegleb BP, Bitz CM, Lin SJ, Zhang MH (2006) The formulation and atmospheric simulation of the Community Atmosphere Model version 3 (CAM3). *J Climate* 19 (11):2144-2161
- Comiso JC (2002) A rapidly declining perennial sea ice cover in the Arctic. *Geophys Res Lett* 29 (20):- . doi:Artn 1956
Doi 10.1029/2002gl015650
- Curry JA, Schramm JL, Perovich DK, Pinto JO (2001) Applications of SHEBA/FIRE data to evaluation of snow/ice albedo parameterizations. *J Geophys Res-Atmos* 106 (D14):15345-15355
- Eisenman I, Wettlaufer JS (2009) Nonlinear threshold behavior during the loss of Arctic sea ice. *P Natl Acad Sci USA* 106 (1):28-32. doi:DOI 10.1073/pnas.0806887106
- Gordon HB, OFarrell SP (1997) Transient climate change in the CSIRO coupled model with dynamic sea ice. *Mon Weather Rev* 125 (5):875-907
- Graversen RG, Mauritsen T, Tjernstrom M, Kallen E, Svensson G (2008) Vertical structure of recent Arctic warming. *Nature* 451 (7174):53-U54. doi:10.1038/nature06502
- Hall A (2004) The role of surface albedo feedback in climate. *J Climate* 17 (7):1550-1568
- Hibler WD, Hutchings JK, Ip CF (2006) Sea-ice arching and multiple flow states of Arctic pack ice. *Ann Glaciol* 44:339-344
448
- Hilmer M, Jung T (2000) Evidence for a recent change in the link between the North Atlantic Oscillation and Arctic sea ice export. *Geophys Res Lett* 27 (7):989-992
- Holland MM, Bitz CM (2003) Polar amplification of climate change in coupled models. *Clim Dynam* 21 (3-4):221-232. doi:10.1007/s00382-003-0332-6
- Holland MM, Bitz CM, Hunke EC, Lipscomb WH, Schramm JL (2006) Influence of the sea ice thickness distribution on polar climate in CCSM3. *J Climate* 19 (11):2398-2414
- Holland MM, Bitz CM, Weaver AJ (2001) The influence of sea ice physics on simulations of climate change. *J Geophys Res-Oceans* 106 (C9):19639-19655
- Johannessen OM, Shalina EV, Miles MW (1999) Satellite evidence for an Arctic sea ice cover in transformation. *Science* 286 (5446):1937-1939
- Kwok R (2009) Outflow of Arctic Ocean Sea Ice into the Greenland and Barents Seas: 1979-2007. *J Climate* 22 (9):2438-2457. doi:Doi 10.1175/2008jcli2819.1
- Kwok R, Rothrock DA (1999) Variability of Fram Strait ice flux and North Atlantic Oscillation (vol 104, pg 5177, 1999). *J Geophys Res-Oceans* 104 (C10):23615-23615
- Kwok R, Rothrock DA (2009) Decline in Arctic sea ice thickness from submarine and ICESat records: 1958-2008. *Geophys Res Lett* 36:-. doi:Artn L15501
Doi 10.1029/2009gl039035
- L'Heveder B, Houssais MN (2001) Investigating the variability of the Arctic sea ice thickness in response to a stochastic thermodynamic atmospheric forcing. *Clim Dynam* 17 (2-3):107-125
- Maykut GA (1982) Large-Scale Heat-Exchange and Ice Production in the Central Arctic. *J Geophys Res-Oc Atm* 87 (Nc10):7971-7984
- Rind D (1987) The Doubled Co2 Climate - Impact of the Sea-Surface Temperature-Gradient. *J Atmos Sci* 44 (21):3235-3268
- Rossow WB, Duenas EN (2004) The International Satellite Cloud Climatology Project (ISCCP) Web site - An online resource for research. *B Am Meteorol Soc* 85 (2):167-172. doi:Doi 10.1175/Bams-85-2-167
- Rothrock DA, Yu Y, Maykut GA (1999) Thinning of the Arctic sea-ice cover. *Geophys Res Lett* 26 (23):3469-3472
- Soden BJ, Held IM (2006) An assessment of climate feedbacks in coupled ocean-atmosphere models. *J Climate* 19 (14):3354-3360

- Soderkvist J, Bjork G (2004) Ice thickness variability in the Arctic Ocean between 1954-1990, results from a coupled ocean-ice-atmosphere column model. *Clim Dynam* 22 (1):57-68. doi:DOI 10.1007/s00382-003-0363-z
- Stefan J (1890) Über die Theorie der Eisbildung. *Monatshefte für Mathematik und Physik* 1 (1):1-6. doi:citeulike-article-id:7091224
- Stroeve J, Holland MM, Meier W, Scambos T, Serreze M (2007) Arctic sea ice decline: Faster than forecast. *Geophys Res Lett* 34 (9). doi:10.1029/2007GL029703
- Thorndike AS (1992) A Toy Model Linking Atmospheric Thermal-Radiation and Sea Ice Growth. *J Geophys Res-Oceans* 97 (C6):9401-9410
- Tietsche S, Notz D, Jungclaus JH, Marotzke J (2011) Recovery mechanisms of Arctic summer sea ice. *Geophys Res Lett* 38 (2):L02707. doi:10.1029/2010gl045698
- Tucker WB, Weatherly JW, Eppler DT, Farmer LD, Bentley DL (2001) Evidence for rapid thinning of sea ice in the western Arctic Ocean at the end of the 1980s. *Geophys Res Lett* 28 (14):2851-2854
- Vavrus SJ (1999) The response of the coupled arctic sea ice-atmosphere system to orbital forcing and ice motion at 6 kyr and 115 kyr BP. *J Climate* 12 (3):873-896
- Webb MJ, Senior CA, Sexton DMH, Ingram WJ, Williams KD, Ringer MA, McAvaney BJ, Colman R, Soden BJ, Gudgel R, Knutson T, Emori S, Ogura T, Tsushima Y, Andronova N, Li B, Musat I, Bony S, Taylor KE (2006) On the contribution of local feedback mechanisms to the range of climate sensitivity in two GCM ensembles. *Clim Dynam* 27 (1):17-38. doi:10.1007/s00382-006-0111-2
- Verlinde J, Harrington JY, McFarquhar GM, Yannuzzi VT, Avramov A, Greenberg S, Johnson N, Zhang G, Poellot MR, Mather JH, Turner DD, Eloranta EW, Zak BD, Prenni AJ, Daniel JS, Kok GL, Tobin DC, Holz R, Sassen K, Spangenberg D, Minnis P, Tooman TP, Ivey MD, Richardson SJ, Bahrmann CP, Shupe M, DeMott PJ, Heymsfield AJ, Schofield R (2007) The mixed-phase Arctic cloud experiment. *B Am Meteorol Soc* 88 (2):205-+. doi:Doi 10.1175/Bams-88-2-205
- Winton M (2006) Surface albedo feedback estimates for the AR4 climate models. *J Climate* 19 (3):359-365
- Wyser K, Jones CG, Du P, Girard E, Willen U, Cassano J, Christensen JH, Curry JA, Dethloff K, Haugen JE, Jacob D, Koltzow M, Laprise R, Lynch A, Pfeifer S, Rinke A, Serreze M, Shaw MJ, Tjernstrom M, Zagar M (2008) An evaluation of Arctic cloud and radiation processes during the SHEBA year: simulation results from eight Arctic regional climate models. *Clim Dynam* 30 (2-3):203-223. doi:10.1007/s00382-007-0286-1
- Zhang JL, Rothrock D, Steele M (2000) Recent changes in Arctic sea ice: The interplay between ice dynamics and thermodynamics. *J Climate* 13 (17):3099-3114

Figures

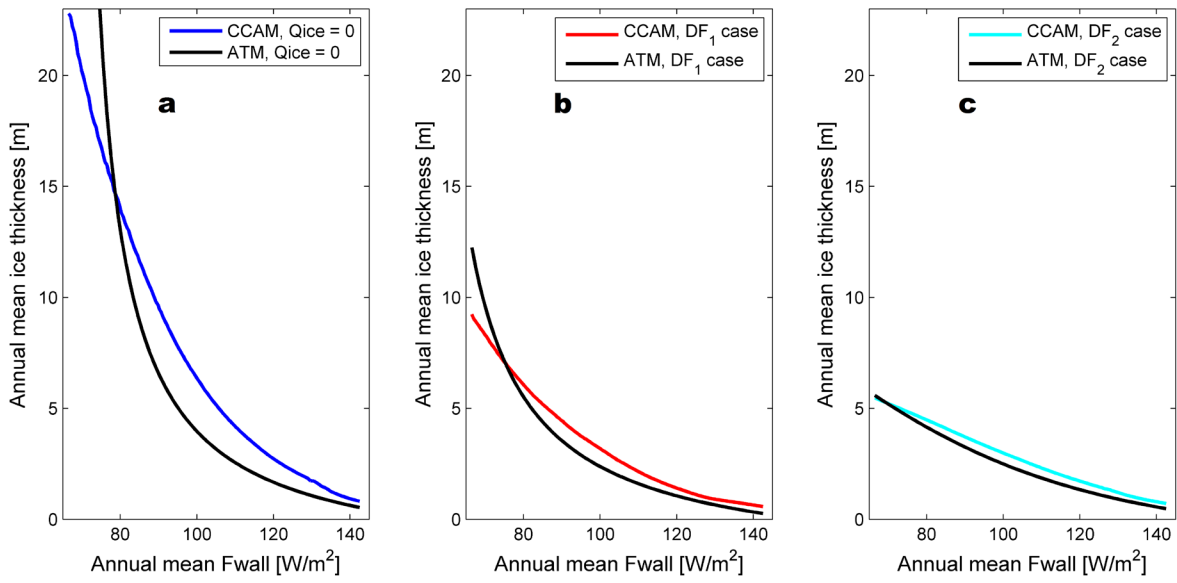


Fig. 1 Dependence of annual mean ice thickness H_{ice} on the annual mean energy advection in the atmosphere, F_{wall} , for the ATM and CCAM models with a) no ice export, b) constant volume export (DF_1 case) and c) constant ice divergence (DF_2 case). The different colors of the CCAM curves are used for reference in Fig. 2

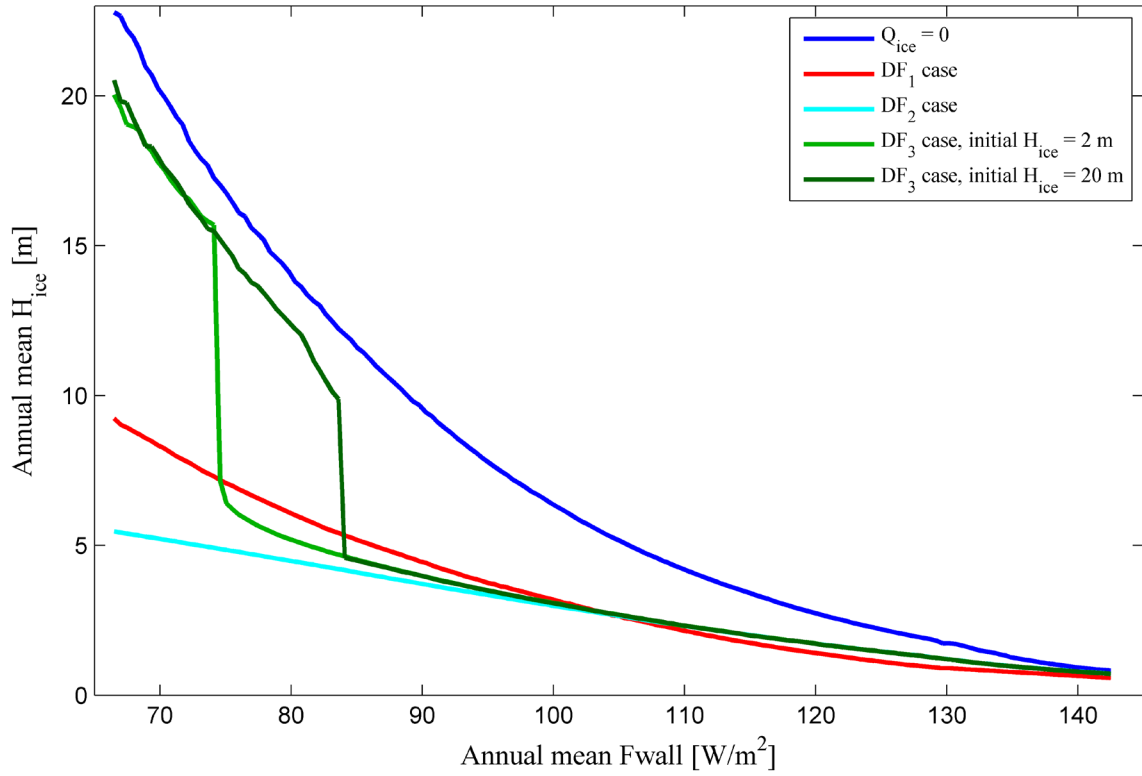


Fig. 2 Dependence of annual mean ice thickness H_{ice} on the annual mean energy advection in the atmosphere, F_{wall} , for the dynamic DF_3 case (see Appendix for details) with two different initial conditions of ice thickness (green curves). The other curves are identical to the CCAM curves in Fig. 1

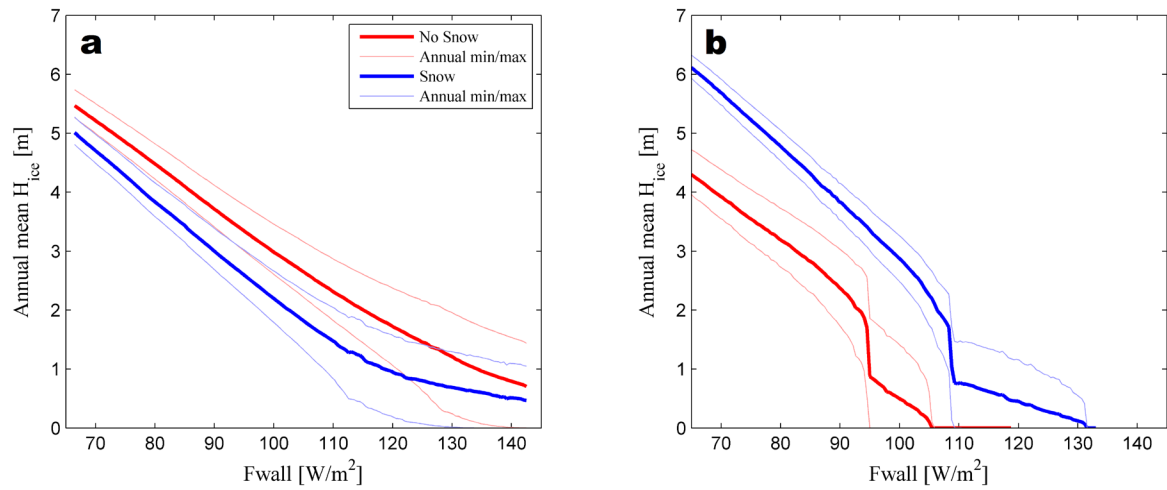


Fig. 3 Dependence of annual mean ice thickness H_{ice} on the annual mean energy advection in the atmosphere, F_{wall} , from the CCAM model and with the constant divergence ice export formulation (DF_2 case) for a) constant albedo and b) albedo dependent on snow and ice characteristics according to (Maykut 1982)

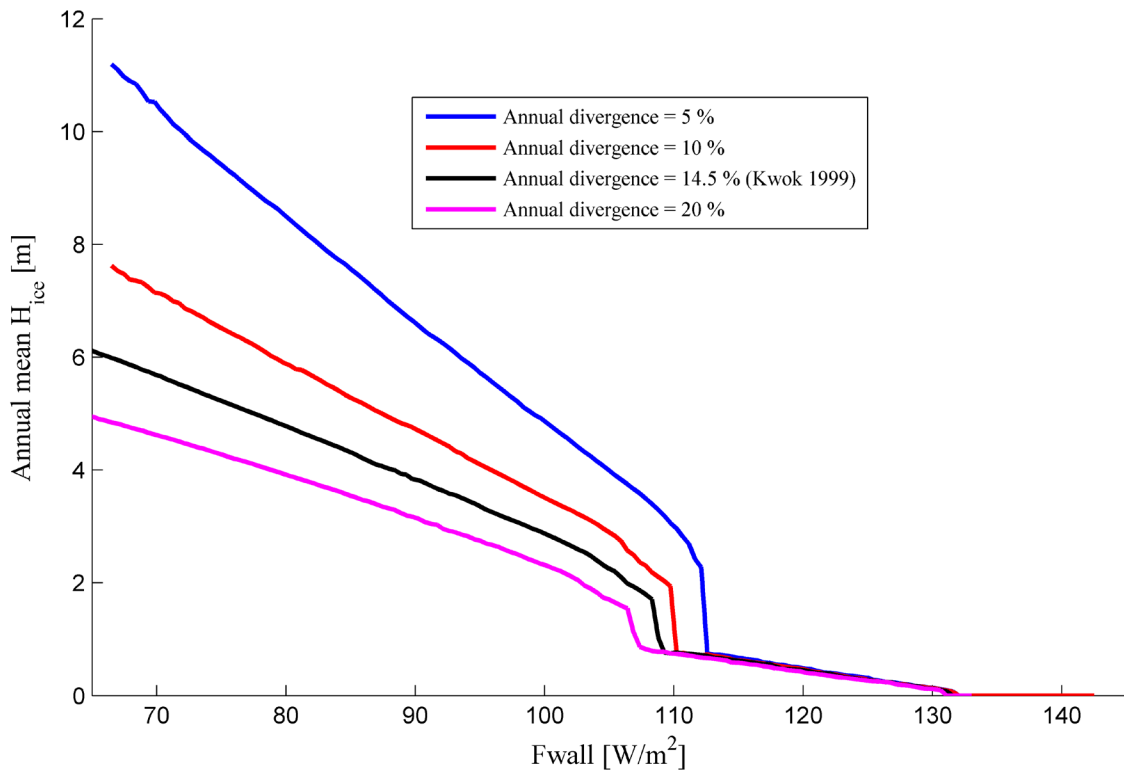


Fig. 4 Dependence of annual mean ice thickness H_{ice} on the annual mean meridional energy advection in the atmosphere, F_{wall} , for different values of the ice divergence given in percent of the Arctic basin area per year

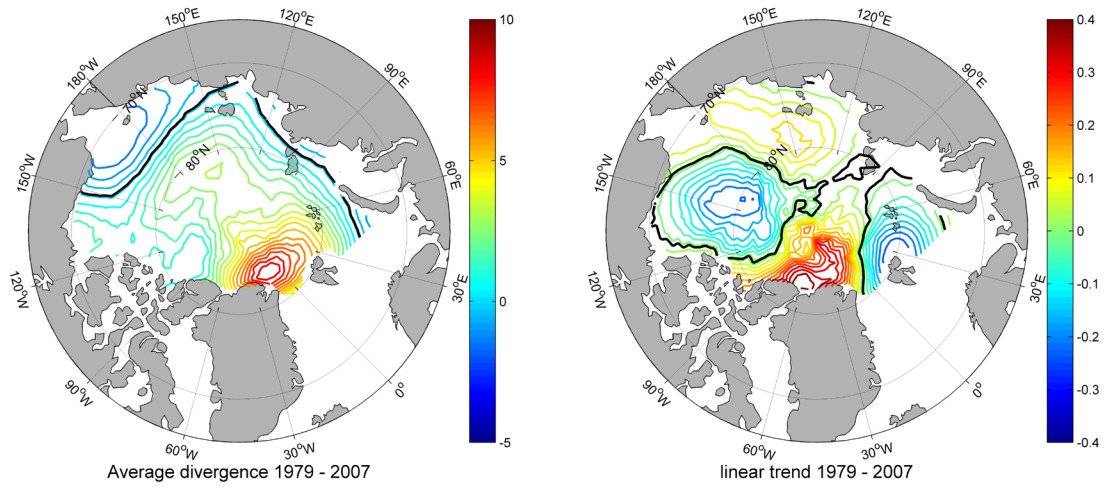


Fig. 5 Divergence fields based on IABP buoy drift data (Rigor, 2002) showing a) the average divergence field in $[10^{-7} \text{ s}^{-1}]$ and b) the linear trend of ice divergence between 1979 and 2007 in $[10^{-7} \text{ s}^{-1} \text{ year}^{-1}]$. The zero iso-lines are shown in black

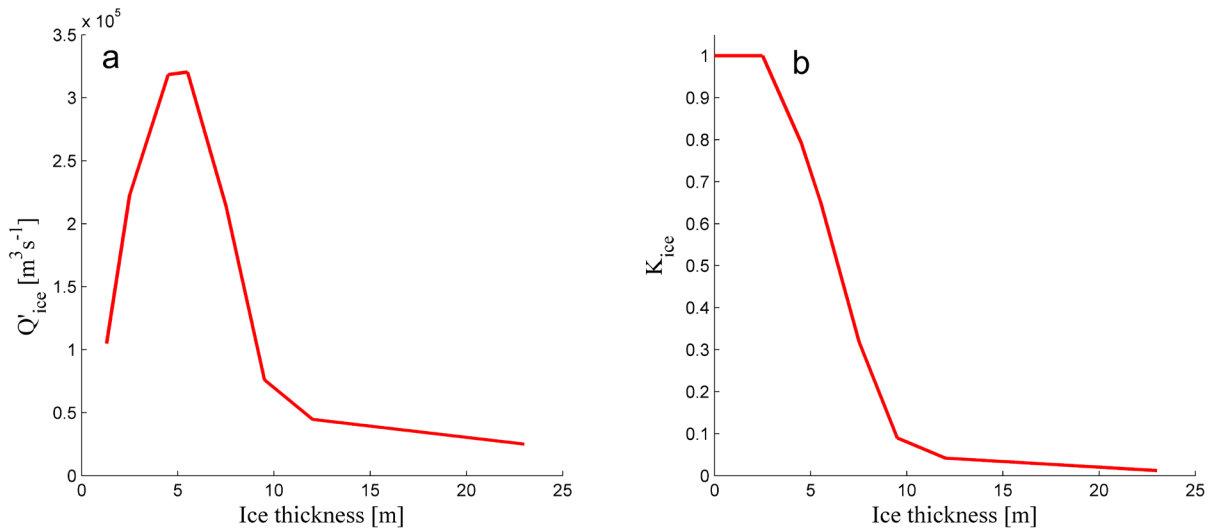


Fig. A1 a) Net Arctic Ocean ice volume export, Q'_{ice} , as a function of ice thickness, approximately reproduced from Hibler and Hutchings (2006). b) Normalized ice thickness factor, K_{ice} used in the DF_3 case, see Eq. (A3)

Tables

Table 1. Definitions and parameter values for the ATM.

H_{ice}	Annual mean ice thickness	Variable
T	Winter mean ice surface temperature [$^{\circ}\text{C}$]	Variable
F_{LU}	Upward longwave radiation from surface	$F_{LU} = AT + B$
A	Coefficient of linearized Stefan-Boltzmann's law	320 W m^{-2}
B	Coefficient of linearized Stefan-Boltzmann's law	$4.6 \text{ W m}^{-2} \text{ }^{\circ}\text{C}^{-1}$
F_{wall}	Atmospheric meridional heat advection	Free forcing parameter
F_{sw}	Summer mean shortwave insolation (80°N)	175 W m^{-2}
F_w	Ocean heat flux	2 W m^{-2}
L	Latent heat of fusion	$3 \cdot 10^8 \text{ J m}^{-3}$
k	Thermal conductivity	$2 \text{ W m}^{-1} \text{ }^{\circ}\text{C}^{-1}$
$n_{w,s}$	Optical depth for winter or summer	2.5 or 3.25
α	Sea ice albedo	0.65
τ	One-half year	182.5 days

Table 2. Model forcing and seasonal dependent parameters^a

	Jan.	Feb.	Mar.	Apr.	May	Jun.	Jul.	Aug.	Sep.	Oct.	Nov.	Dec.
$F_{wall} [\text{W/m}^2]$	118.3	108.5	107.5	92.6	72.6	72.8	72.6	78.3	98.1	97.3	112.3	108.4
$D [10^{-9} \text{ s}^{-1}]$	5.4	5.4	5.3	5.1	3.0	4.3	3.8	3.7	4.3	4.3	5.0	5.7
CF_{high}	0.08	0.09	0.06	0.02	0.01	0.02	0.04	0.04	0.04	0.04	0.05	0.07
CF_{mid}	0.50	0.50	0.49	0.34	0.22	0.25	0.29	0.32	0.34	0.37	0.44	0.49
CF_{low}	0.11	0.10	0.11	0.17	0.20	0.20	0.20	0.20	0.21	0.23	0.16	0.12
α_{snow}	0.85	0.84	0.83	0.81	0.82	0.78	0.64	0.69	0.84	0.85	0.85	0.85
$S_{prec} [\text{mm/day}]$	1	0.9	0.9	0.7	0.7	0.9	1.4	1.6	1.6	1.4	1.1	1.0

^a For additional parameters see (Bjork and Soderkvist 2002).